Recent changes to the biogeochemistry of Muchalat Inlet, B.C., and the implications for HABs

Julia Marks[1]

[1]University of Washington, School of Oceanography

June 2015

ACKNOWLEDGEMENTS

ABSTRACT

The western coast of Vancouver Island, B.C. experienced anomalous events in the late spring and early summer of 2014. A persistent warm sea surface temperature anomaly reached the fjords, as did a massive "flushing" event, replenishing deep fjord basins with oxygenated water (Bond et al. 2014, Rick Keil personal communication). During this same period, a Harmful Algal Bloom (HAB) hit Muchalat Inlet, resulting in a large fish kill (Judd 2014). This study assessed the possibility that the recent HAB was instigated by toxin-producing phytoflagellate cysts that germinated due to the anomalous change in bottom-water conditions. First, a sedimentation rate of approximately 5mm/yr was computed using radiocarbon, and applying this rate to X-ray images of the core, certain sections were qualitatively considered to be varved. Individual sediment layers within the varve couplets were composed of differing amounts of % Organic Carbon and certain metals that were associated with terrigenous runoff. Once sedimentation dynamics were examined, *Alexandrium* spp. cysts and metals abundance were used as a metric for recent changes to the sedimentary record. Cysts were absent below 14 cm, and the highest concentrations were found at the surface. A large spike in manganese was observed at approximately 9 cm below the surface. This was attributed to oxygen penetration of deeper waters, though the spike could not be dated. This study concludes that recently deposited sediments exhibit a favorable environment for cyst germination. Based on these preliminary results, it seems plausible that toxin-producing cysts, which were capable of germinating under anomalously warm and oxic conditions, generated the 2014 HAB.

INTRODUCTION

The glacial history of Vancouver Island, B.C. has left its western coast characterized by sounds and inlets (Dodimead 1984). Many of these inlets have shallow entrances due to the presence of a sill. Beyond the sill exist long, deep basins. This glacially produced bathymetry can often result in a highly stratified water column with nearly anoxic bottom waters. Without deep-water renewal, the rate of oxygen consumption dominates the rate of oxygen replenishment and anoxic near-bottom conditions ensue (Calvert & Pederson, 1993). Additionally, fjords are often sinks for terrigenous organic carbon from seasonal freshwater input (Walsh et al. 2008). Conditions of low dissolved oxygen and seasonal variation often produce a laminar sedimentary record by limiting the amount of bioturbation that can occur and accumulating seasonal layers with alternating composition (Calvert & Pederson 1993). Consequently, a sediment core obtained from a Vancouver Island fjord would plausibly contain laminae exhibiting annual couplets due to seasonality, also called varves.

This aforementioned description of a sediment core from the basin of an anoxic fjord can be seen as a baseline for many of these inlets along the western coast of Vancouver Island. Conversely, recent events impacting the western North Pacific could have made changes to this baseline. Anomalously warm ocean water reached the western coast of North America beginning in spring 2014, resulting in the warmest sea surface anomaly for at least three decades (Bond et al. 2015). This warm anomaly hit the western coast of Vancouver Island around May 2014, and two events were observed in the succeeding months. The first was a massive "flushing" event, where bottom water in many of the fjords was replenished with oxygenated waters (Keil, personal communication). The second was a Harmful Algal Bloom (HAB) near Gold River in Muchalat Inlet that resulted in a large fish kill (Judd 2014).

The timing of this HAB event with the warm anomaly and the "flushing" event leads to the question of whether it was generated by plankton residing in the sediments. Many phytoflagellate species exhibit a dormant cyst phase as a part of their life cycle. After having lived in the photic zone as motile organisms, these plankton species will enter a non-motile cyst phase, where components of the organisms' cell are compressed and encased in a multi-layered wall. These resting cysts then sink through the water column and are deposited in the sediments where they usually stay well preserved for many decades, sometimes centuries (Meksumpun et al. 1994, Kennaway & Lewis 2004). Studies have shown that these cysts are capable of germinating, and subsequently instigating phytoplankton blooms after many seasons of dormancy (Mizushima & Matsuoka 2004, Meksumpun et al. 2005, Cox et al. 2007, Shikata et al. 2007).

Temperature and dissolved oxygen levels are considered to influence the germination ability of phytoflagellate cysts (Mizushima & Matsuoka 2004, Meksumpun et al. 2005, Shikata et al. 2007). The impact of each of these factors on germination ability is still a topic of debate, though it would seem that once cysts have germinated they are more likely to survive and instigate a bloom in warmer conditions (Shikata et al. 2007). Hence, the warm anomaly that increased water temperatures, and the flushing event that increased dissolved oxygen levels in the near-bottom environment could have changed the conditions in Muchalat Inlet, making it a more conducive environment for cyst germination.

Along the west coast of North America there are two common toxin-producing phytoflagellates that produce resting cysts. One is a genus of dinoflagellate, *Alexandrium*, which is capable of producing a saxitoxin that leads to Paralytic Shellfish Poisoning (Horner et al. 1997). The other is a species of radiophyte, *Heterosigma Akashiwo*, which causes pervasive red

tide that leads to massive fish kills (Shikata et al. 2007). Additionally, *H. Akashiwo* was recorded as one of the main phytoplankton in a 2006 HAB on Vancouver Island (Almeda et al. 2010). The presence of these two cyst-forming plankton in the NE Pacific supports the possibility that the HAB observed in June 2014 was perpetrated by germinated cysts from the sediments.

This study examined a sediment core from the deep basin of Muchalat Inlet, near Gold River, in an attempt to capture recent changes to the sedimentary record associated with the June 2014 HAB. In order to see changes to the record, however, a baseline study was also conducted. While much is known about the oceanographic processes that govern fjords, Muchalat Inlet is an understudied area. Therefore, the initial focus of this study was to establish the sedimentation dynamics of Muchalat Inlet. To achieve this, a sedimentation rate was estimated using radiocarbon measurements of terrestrial macrofossils. In addition, X-ray images of sediment cores were examined for annual varve-couplets, or alternating sediment layers indicating seasonality. Individual sediment layers were also tested for metals abundance and % Organic Carbon (OC) to link distinct layers with seasonality.

With a baseline of the sedimentation dynamics of Muchalat Inlet, we examined recent changes to the sedimentary record that could be associated with the 2014 HAB. Concentrations of *Alexandrium* spp. cysts were enumerated at incremental depths in a sediment core. *Alexandrium* spp. was selected because many *Alexandrium* spp. records have been reconstructed along the NE Pacific coast, and the method for enumerating *Alexandrium* spp. cysts is well established (Yamaguchi et al. 1995, Mudie et al. 2002, Cox et al. 2007, Feifel et al. 2011).

Though the precise species that composed the 2014 HAB went unreported, it is known that this species killed over 44,000 salmon (Judd 2014). *Alexandrium* spp. does not produce a toxin that kills fish, however, it is plausible that the bloom was composed of *H. Akashiwo* as this

species does implicate fish kills and is a common taxa in the area (Haigh & Taylor 1990, Almeda et al. 2010). Using the knowledge that both taxa (*Alexandrium* spp. and *H. Akashiwo*) form resting cysts and are more likely to germinate under warmer conditions with higher levels of dissolved oxygen, the *Alexandrium* spp. cyst record could be associated with an *H. Akashiwo* cyst record. Therefore, changes to *Alexandrium* spp. cyst concentrations were used as an indicator of changes in *H. Akashiwo* cyst concentrations.

The sediment core was also examined for recent changes that could reflect shifts to the near-bottom conditions of Muchalat Inlet, making it more conducive for cyst germination. This study measured a proxy for dissolved oxygen levels to try to capture the recent flushing event. The sediment core was tested for metals that would indicate a change in redox conditions. The boundary between anoxic and oxic sediments can be detected through the change in abundance of specific metals that precipitate or dissolve depending on the redox conditions (Libes 1992). Hence, the abundance of certain metals was tested throughout the core to compare recently deposited sediments to deeper ones from the baseline. Changes in abundance were used to visualize recent changes to the normally anoxic metal profile.

METHODS

Study Site

Nootka Sound is a large embayment on the west side of Vancouver Island. Sitting at approximately 49° North and 126° West, the sound comprises three main inlets. One, Muchalat Inlet is a long, narrow, and deep fjord, approximately 48 km long with an average width of 1.5 km and a maximum depth of 385 m (Dodimead, 1984). The inlet also contains two sills near its convergence with Nootka Sound. The bathymetric profile created by this fjord displays a deep basin, conducive of minimal deep circulation. Based on these assumptions, Muchalat Inlet was

hypothesized to be an ideal setting for obtaining a laminar sediment core with an intact stratigraphy.

Data Collection

Two sediment cores were collected from the R/V Thomas G. Thompson in December 2014. In an attempt to obtain the most well preserved cores, the cores were sampled from the deepest part of the Muchalat basin, at approximately 348 m water depth (Fig. 1). Two sediment cores were collected using two different coring devices. One was obtained using a spade-arm box corer that collects 60 cm-long cores, and the other using a 180 cm-long Kasten core.

Due to the very fine composition of the Muchalat basin sediment, both the box and the Kasten corer over-penetrated, and the surface was therefore not captured in the core barrels. However, the surface sediment was detectable above the upper limit of the actual box because of the presence of a thin film of sulfur-reducing bacteria, tentatively identified as *Thioploca* spp. Using this thin film as a marker, an approximately 1 cm-thick layer of surface sediment was scraped off and saved separately. Both cores were partitioned and preserved using an X-Ray tray and sample bags, however the methods for partitioning varied slightly.

A 60 cm-long X-Ray tray and a 60 cm-long cylinder with a 6-inch diameter were simultaneously pushed into the box core. The X-Ray tray was capped, labeled and refrigerated until ready for imaging. The cylinder was passed through a 6-inch extruder and partitioned at 1 cm increments for the first 10 cm, then 2 cm increments for the bottom 50 cm.

The sediment inside the Kasten core was kept in place by a neoprene block pushed in at the top and a one-way valve that acted as a platform on the bottom. The core was then laid out horizontally and the removable fourth side was unscrewed. Due to the high water content at the top of the barrel, the first 29 cm of sediment below the surface had slumped and was thus

impossible to partition. This top section could therefore only be homogenized and collected into a bag. Starting at 29 cm below the core top, X-ray trays, 30 cm long, were pushed into the exposed sediment. The fourth side of the X-Ray tray was slid into place and each tray was removed from the barrel, capped, labeled and stored in the refrigerator for later imaging. The remaining sediment in the barrel was then partitioned using thin metal plates. The first 30 cm, from 29-59 cm below the top of the core, were partitioned at 1 cm increments and collected into sample bags. The rest of the core was divided at 2 cm increments.

Oxygen levels were detected using a Seabird SBE 911plus CTD rosette. The rosette contained both an oxygen sensor and Niskin bottles that collected water samples at various depths. A CTD cast was deployed close to the sampling site and an oxygen-depth profile was produced using the mounted sensor. The deepest oxygen measurement was recorded as an indicator of near-bottom oxygen conditions for the basin.

Fig. 1. Map of Muchalat Inlet and Nootka Sound, Vancouver Island, B.C. The sediment core collection site is marked in red.

Data Processing

In order to effectively analyze the sediment core, data processing had to occur in a specific order. First, the core had to be imaged using a Computerized Tomography Scan. The visual information from these images determined the samples that would be used to date the core. Once these two dataset were acquired, the test for metals and the reconstruction of an *Alexandrium* spp. cyst record could be accomplished.

Computerized Tomography Scan

The X-ray trays from the box core and the Kasten core were scanned through a Computerized Tomography (CT) Scan at Via Radiology, Seattle, WA. The scans produced X-ray images of the cores that exposed the varying densities of sediment. Less dense sections of the core displayed a darker shade while denser sections displayed a lighter shade. Using these visual cues, the core images were examined for varves, or couplets of alternating shade layers that represent annual seasonality. Terrestrial plant material chosen for Carbon-14 dating were taken from depths that displayed laminar sediment.

Furthermore, the X-ray tray from the box core was disassembled and subsampled based on the alternating shades of laminated sediment. One sample representative of the darker shaded material was extracted from 28 cm below the surface and another sample, representative of the lighter shaded sediment, from 25 cm below the surface. These two sediment samples were tested for metals and % Organic Carbon (OC).

Carbon-14

The radioactive isotope, Carbon-14, was used to date the two sediment cores. Radiocarbon can date modern sediments (post-1950) due to the aboveground Nuclear weapon tests that occurred in the late 1950s and early 1960s. These tests led to a rapid and immense increase in atmospheric ^{14}C, as well as a subsequent fall after 1963 when an atmospheric nuclear test ban treaty was implemented (Wild et al. 2000). This rapid rise and fall of atmospheric ^{14}C became known as the "bomb peak," and can be used to produce a calibration curve, linking Radiocarbon content with a calendar year.

Five depths from the two cores were dated. The two samples from the box core were from 13 and 19 cm below the top of the core, and the three samples from the Kasten core were

extracted from 30, 40, and 45 cm below the core top. The two sets of samples were analyzed

separately, and compared in order to establish an accurate sedimentation rate. For each depth, a

subsample of sediment was sieved and examined for terrestrial organic material. Approximately

0.5-2 mg of terrestrial organic material was collected into labeled jars and dried overnight. Each

sample was then run through an Acid-Base-Acid protocol established by Brock et al. 2010. All

samples were submerged in 1M HCl and heated for 20 minutes at 80° C. After being rinsed with

MiliQ water, the samples were submerged in 0.2M NaOH and heated again at 80° C for 20

minutes. This was repeated with 1M HCl, then rinsed and dried overnight.

After the Acid-Base-Acid treatment was complete the samples were sent to DirectAMS,

an Accelerator Mass Spectrometry Lab in Bothell, WA, for radiocarbon dating. The results from

dating were expressed as a Fraction Modern, and were then calibrated for age using the

chronology technique established by the [14]Chrono Centre from Queen's University Belfast

(CALIBomb, Reimer et al. 2004). This method used the INTCal13 radiocarbon age calibration

curve with the Northern Hemisphere Zone 1 (NHZ1) compilation.

Cysts: processing and enumeration

The method for cyst extraction and identification was described by Yamaguchi et al.

(1995) and adapted by Kirsten Feifel, a former Ph.D. student in the Lessard Lab in at the School

of Oceanography, University of Washington.

Seven of the core sections were examined for cysts. For each location, sediment was

homogenized and subsampled. Five cm^3 of homogenized sample was diluted with filtered

seawater to a 1:5 ratio, sonicated, and then sieved through a 90μm and a 20μm filter. 0.75 mL of

Formalin was added to the sieved sample (extracted cysts) and the new solution was set on a rack

for two hours. After this time the Formalin was aspirated and the samples were refrigerated in

methanol for two days. The fixed sample was then stained with Primuline, which caused the cellulose in the cyst cell to fluoresce, and left for an hour before being rinsed.

Once a sample was rinsed, a 1 mL subsample was spread onto a Sedgwick-Rafter counting chamber and counted. Cysts were visualized using a standard microscope with epifluorescence and specific excitation filters to excite the Primuline stain (one filter with a 420-490nm bandwidth and the other with a 330-380nm bandwidth). The entire slide was examined for *Alexandrium* spp., as well as another genus of dinoflagellate, *Scrippsiella* spp., and other groups of organic material that acted as controls throughout the study (when dinoflagellate cysts were absent in a sample, the presence of the other organic material confirmed the accuracy of the aforementioned methods). Fig. 2 shows an example of an *Alexandrium* spp. cyst under white light and epifluorescence.
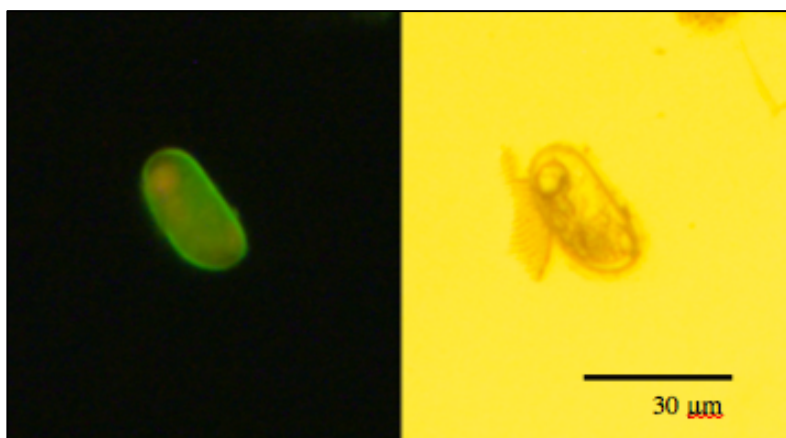

Fig. 2. Two pictures of the same *Alexandrium* spp. cyst found in the surface sediment at the sampling site. The left image shows the cyst under eipfluorescence while the image on the right shows the same cyst under white light. The well-defined cyst wall and the globular appearance within the cyst are two of the identifying traits of the *Alexandrium* spp.

Metals

Sixteen samples spanning the length of the core, as well as the two samples from the X-ray trays, were tested for abundance of metals by ICP-AES (Inductively Coupled Argon Plasma Atomic Emission Spectroscopy). The EPA-3050b method was used to process each sample, digesting them through a HNO_3, H_2O_2 and HCl treatment (USEPA 1996). The digested samples were run through a model 61E Thermo Scientific ICP-AES instrument. It is important to note that the dried samples were not washed before being tested for metals, so the measurement of metal abundance could include formerly dissolved forms from evaporated pore water. Among the metals tested for, those relevant to this study included Mn, Al, S, Ca, and Na.

Organic Carbon

Loss on ignition was measured for 15 samples throughout the box core, as well as the two samples from the X-ray tray (each taken from a single laminated sediment layer). Each dried sample was weighed, and placed in an oven at 400° C for 12 hours. After being combusted, each sample was re-weighed and the difference in final and initial weights was used as a proxy for %OC (Schumacher 2002). This was done using the equation below. It is important to note that the samples had been dried prior to this analysis in an oven at 140° C. A small loss in volatile organic carbon could have occurred due to the high temperature of the oven.

$$\frac{(initial\ mass - final\ mass)}{initial\ mass} \times 100\% = \%\ Loss\ on\ Ignition \cong \%\ OC$$

RESULTS

CT Scans

 The CT scan images of the Kasten core (from 29-59 cm) and the box core were synchronized based on laminae (Fig. 3). In the box core, the section of sediment between approximately 5 cm and 48 cm below the top of the core displayed well-defined laminae. The layers of sediment characterized by lighter shading denoted denser material and the darker shaded layers of sediment signified less dense material.
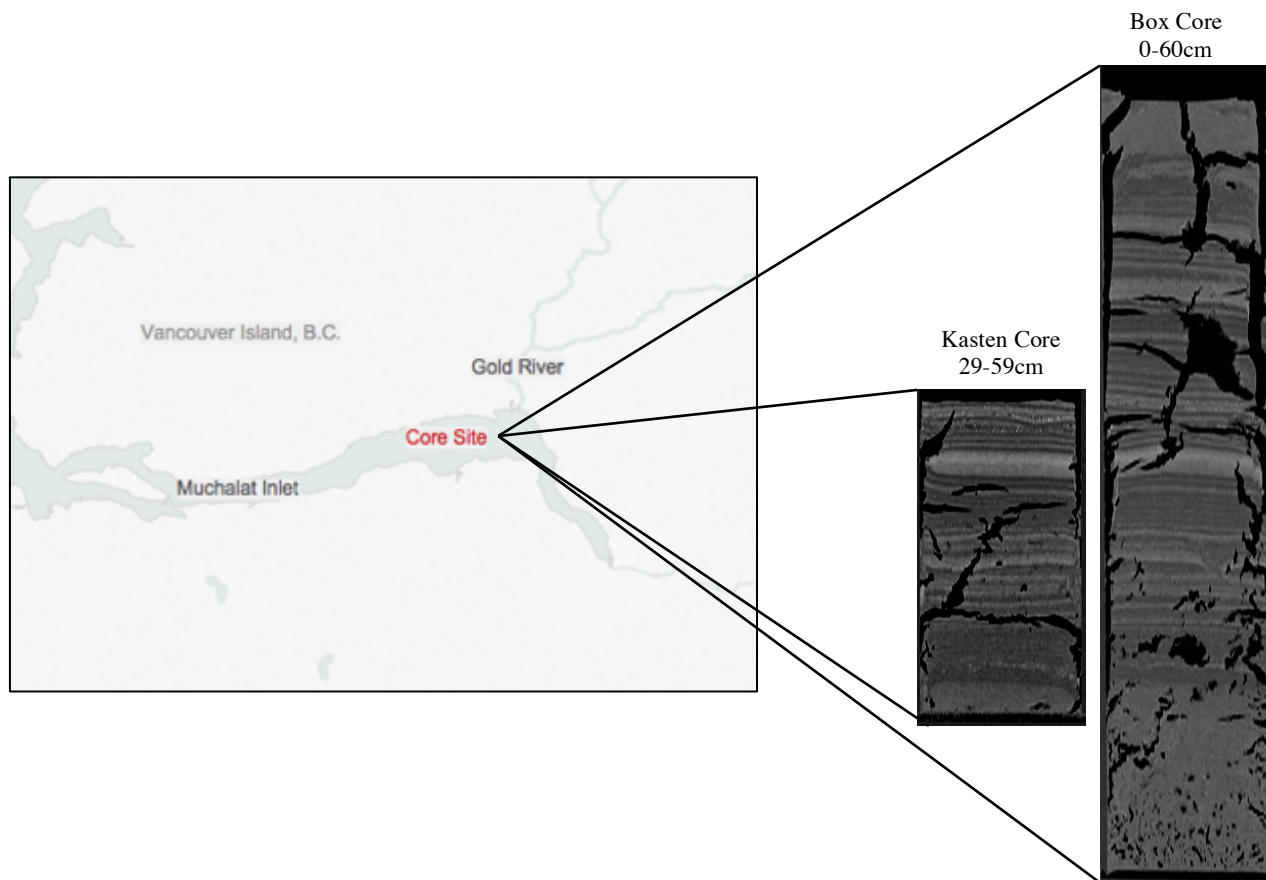

Fig. 3. CT scanned images of the two sediment cores collected at the Muchalat sampling site: the right image is of the box core and left shows a section of the Kasten core from 29-59cm. The two cores were easily synchronized based on their similar lamination patterns.

Carbon -14

Two depths from the box core and three from the Kasten core were subsampled for terrestrial plant macrofossils that could be dated by ^{14}C. The radiocarbon content of each sample was associated with two dates, one on either side of the bomb curve (Fig. 4). Figures 5a and 5b display both dates for each sample. A linear regression was then produced for each core by selecting one date for each depth, and the slope of the regression line was interpreted as the sedimentation rate (Fig. 5c, 5d). For the box core, the two dates with the highest probability were selected and produced a sedimentation rate of 0.5 cm/yr (Fig. 5c).

The Kasten core linear regression was produced using only two points, one from 30 and the other from 40 cm below the core top. The radiocarbon data from 45 cm was removed because it was considered a reversal. This conclusion was made based on the depth of the sample taken, as it is possible that this organic material was from a depth that did not display the laminations from the X-ray image. Although the X-ray tray exhibited laminae downcore until approximately 48 cm, the sediment from the cylinder, used for extracting radiocarbon subsamples, could have been slightly offset. From the two shallower depths of the Kasten core, a sedimentation rate of approximately 0.5 cm/yr was produced (Fig. 5d). The rates of deposition computed from the two plots were extremely similar and thus give confidence as to the sedimentation dynamics of the Muchalat basin near its deepest point.

A sedimentation rate was the only characteristic that was confidently determined from these ^{14}C results. Due to the limited number of data points obtained, as well as the over-penetration of the core, a more accurate chronology could not be determined.
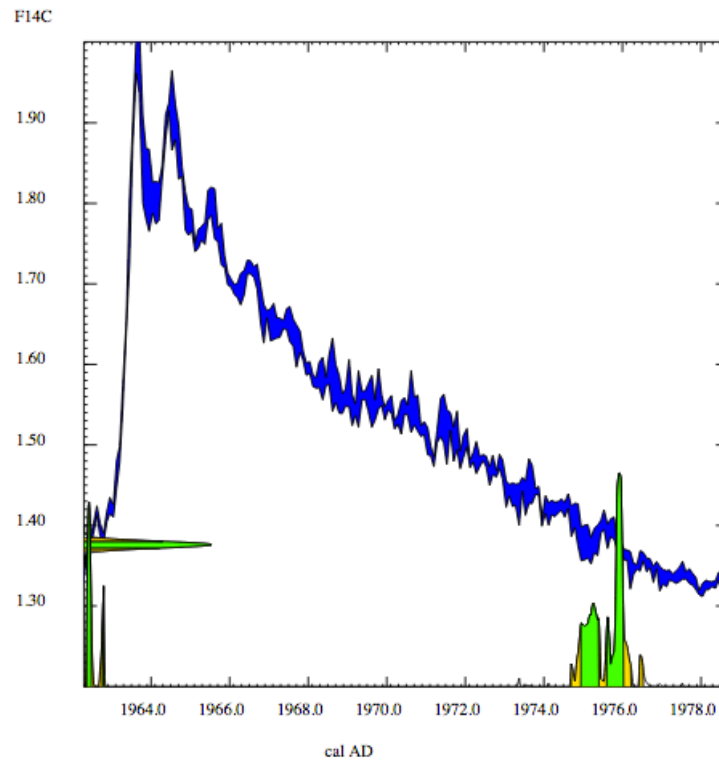
Box Core: 19 cm below core top

Fig. 4. Calibration curve produced by [14]Chronos (CALIBomb). This plot is of radiocarbon content from 19cm below the top of the box core. This particular sample had a fraction modern value of 1.3761 and a standard error of 0.0041. The two dates associated with this sample, displayed on Fig. 5a, are 1975 and 1962.
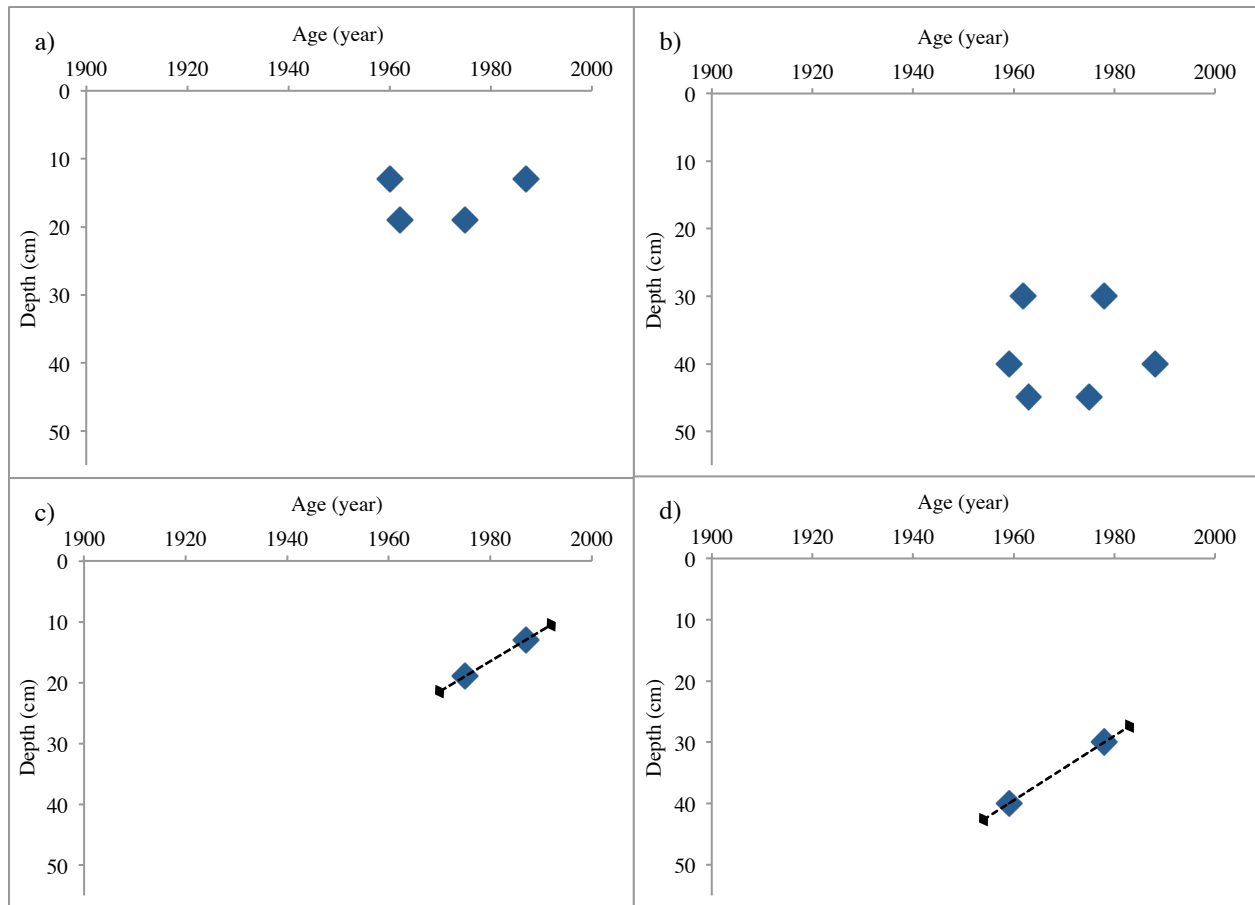
Fig. 5. Four depth profiles of calibrated ^{14}C data, two from each sediment core. 5a) and 5c) are plots produced from the two box core samples, and 5b) and 5d) show data from the three samples from the Kasten core. 5a) and 5b) display all possible dates for each depth, including their corresponding probabilities. 5c) and 5d) show the linear regression produced from selected dates at each depth, the only exception being the deepest point on the Kasten core plot (5d), which was considered a reversal and removed. Linear regression for 5c): depth = -0.5263(age) + 1071.1, for 5d): depth = -0.5(age) + 1006.5.

Sedimentation dynamics: significance of the visual layers

The sedimentation rate found from the radiocarbon results was used to determine whether the laminae displayed in the CT scan images could be classified as varves. The sedimentation rate of approximately 0.5 cm/yr was used to calculate an empirical number of sediment layers for each section counted, and this ideal number was compared to the measured number (Table 1). To classify as varves, a couplet of light and dark sediment layers would have to equate to one year of sediment, thus a thickness of 0.5 cm in Muchalat Inlet. Based on this, two distinct sediment

layers should have been seen for a 1 cm section of the core. The average value calculated was approximately 1.57 layers for each cm of sediment.

The two samples representing the light and dark shades of sediment had differing concentrations of sodium, sulfur, calcium and %OC (Fig. 6). Each of these variables displayed a higher abundance in the dark sediment layer and a smaller abundance in the light sediment layer. In order to compare metal concentrations to one another, each were expressed as a ratio to the concentration of aluminum. Aluminum is a very stable, lithogenic element that can be used to compare metals to each other as well as to the average crustal composition (Wedephol 1971).

Table 1. The observed number of visual sediment layers from 4 sections of the box core. The number of observed layers was based on the laminae displayed from the CT scan image. The theoretical number of layers was computed based on the 0.5 cm/yr sedimentation rate estimated from radiocarbon dating, and an average number of layers was calculated based on the observed data.

Core Section (Box core)	Thickness (cm)	Empirical # of layers	Observed # of layers
	2.6	10	9
	3.6	14	11
	3.6	14	13
	3.6	14	9
Average	*3.35*	*13*	*10.5*

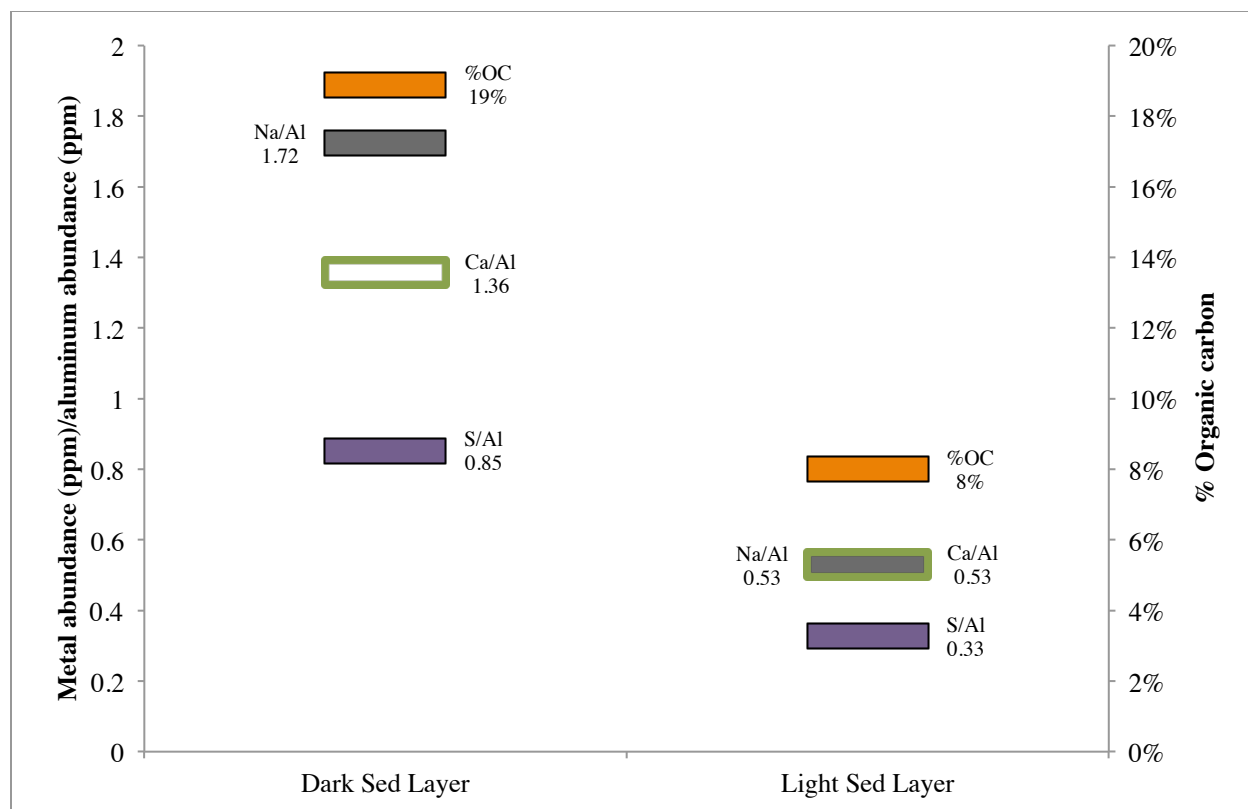| Confirmation of Varves	Thickness (cm)	Empirical # of layers	Observed # layers based off of average from above
Average from above applied to one year of deposition	**0.5**	**2**	**1.57**

Fig. 6. Difference in %OC and the ratio of Na, Ca, and S to Al between the dark (lower density) and light (higher density) varves extracted from the X-ray tray. Elemental abundances relative to aluminum allow comparison to the average crustal composition.

Manganese and Organic Carbon

Manganese was measured in µg/g, or ppm, for 16 samples throughout the box core (Fig. 7). Throughout the core, abundance of Mn ranged from approximately 650 to 18100 ppm. Concentrations of Mn varied widely from the surface to approximately 10 cm below the surface. This section of upper sediment exhibited a spike at 5 cm corresponding with the highest Mn concentration of approximately 18100 ppm. Below this period of variance, Mn concentrations became mostly uniform with an average of approximately 760 ppm. A small increase was detected at 38 cm below the surface where the Mn concentration exceeded 1000 ppm.

Throughout the box core, %OC ranged from ~10-22% with the largest value found at 26 cm below the surface (Fig. 7).
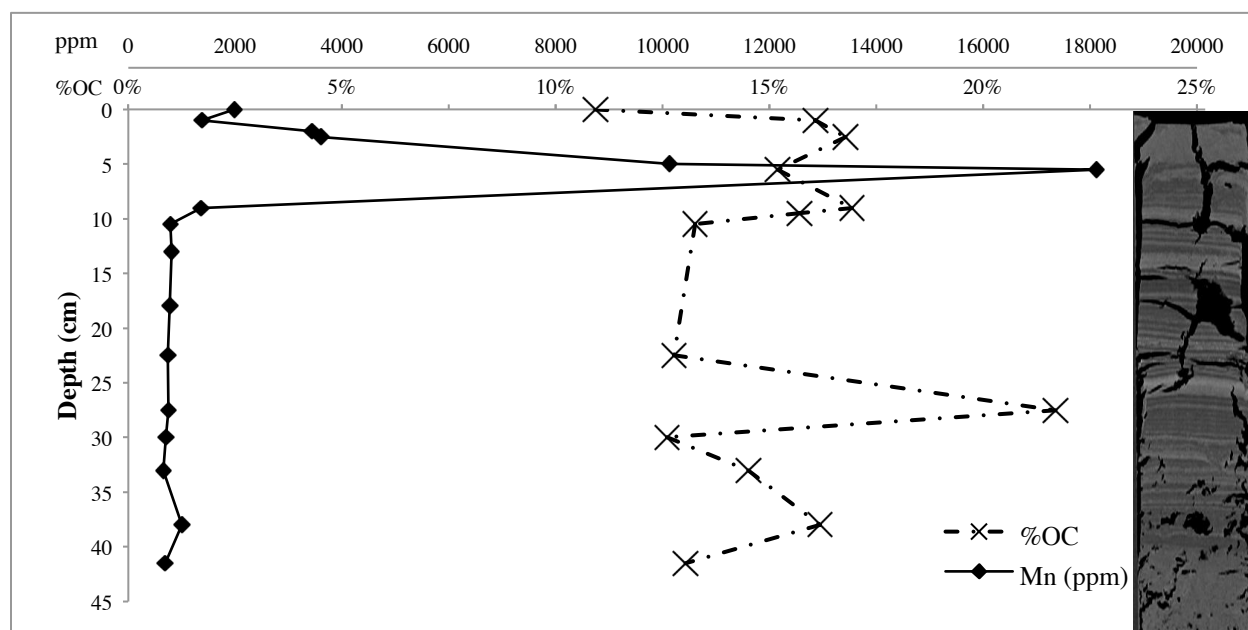

Fig. 7. A depth profile of manganese and %OC throughout the box core.

Cysts

Alexandrium spp. cysts were enumerated throughout the box core (Fig. 8).

Concentrations of *Alexandrium* spp. cysts ranged from 0 to 14 cysts*g_{dry}^{-1}, with the highest

concentrations found in the surface sediments. *Alexandrium* spp. cysts were present at every

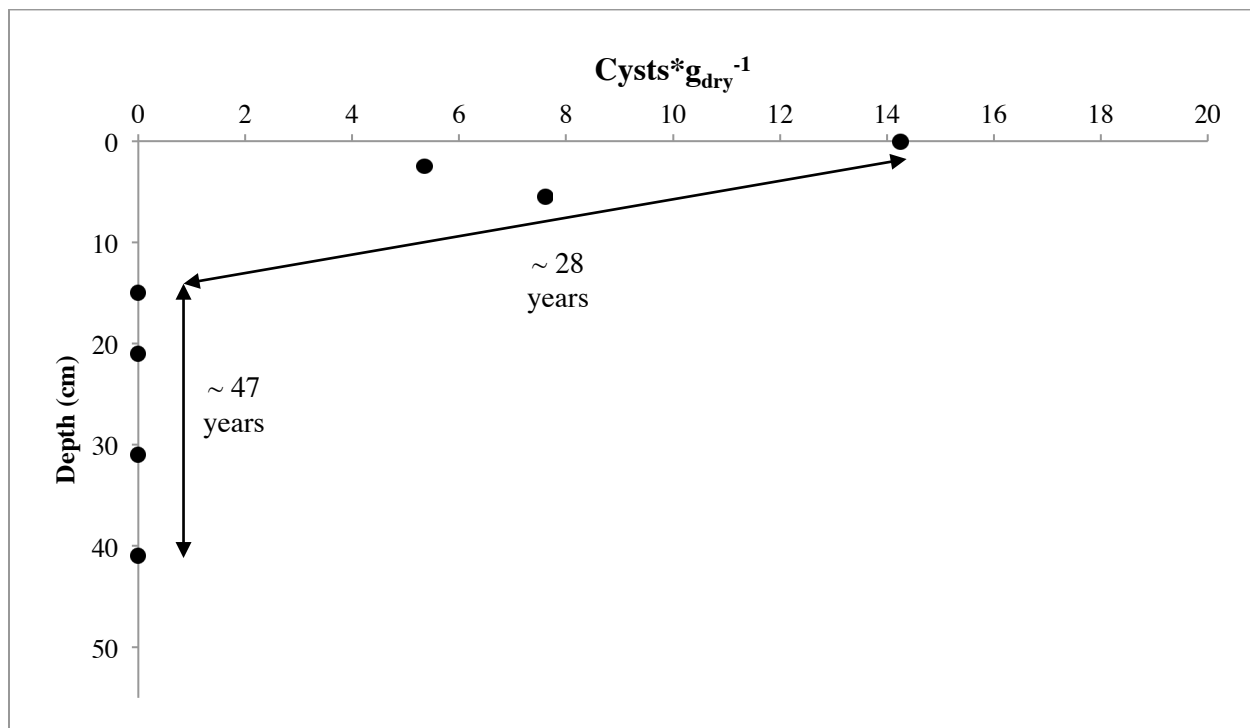depth above 14 cm in the core. Below this depth, *Alexandrium* spp. cysts were not detected.

Fig. 8. Depth profile of *Alexandrium* spp. cysts throughout the box core. The x-axis shows concentration of cysts*g_{dry}^{-1}, and the y-axis displays depth in cm. Due to the uncertainty from the radiocarbon results, an age axis was omitted, however age ranges based on the 0.5 cm/yr sedimentation rate are shown.

DISCUSSION

Varves: Sedimentation Dynamics of Muchalat Inlet

<u>Verification of Varves</u>

The significance of the distinct sediment layers was determined using the sedimentation rate computed from the radiocarbon results in conjunction with the measured frequency of alternating shades. The results from Table 1 show an average of 1.57 layers/cm, while this should empirically be 2 layers/cm based on a sedimentation rate of 0.5 cm/yr. There are many feasible explanations for this difference. First, the difference between measured and empirical values could be attributed to variations in freshwater discharge and annual rainfall from year to year. As seen in Fig. 3, the thickness of the sediment layers varies throughout the core, so annual variation is a plausible explanation for the difference between the observed average and the empirical value.

Secondly, this difference could be based in methodology errors. One possible source of error comprises an omission in sediment layers from the counting method, resulting in an underestimated number of observed layers. This source of error is plausible because the observed average (1.57 layers/cm) was less than the empirical value (2 layers/cm). Another methodology source of error could originate from a miscalculated sedimentation rate. There is a possibility that the sedimentation rate found from the radiocarbon results was not precise because only five samples were dated. Therefore, it is plausible that the 0.5 cm/yr sedimentation rate does not represent the true accumulation rate of Muchalat basin, and thus can be the source of offset between the measured and empirical sediment layers/cm.

Lastly, it is possible that these observed laminae do not indicate annual layering, and therefore are not varves. Although this last explanation is important to note, this study concluded

that the laminae seen can be characterized as varves, or alternating shades specifically

representing annual seasonality. This is a useful tool, as a rough history of the region's

sedimentation can be determined solely based on the visualization of the CT scans.

Sediment Composition: Metals and %OC

To further analyze the sedimentation dynamics, the different shades of sediment were

examined for metals and %OC. Distinctions between the two layers were evident through %OC

and certain metal abundance when expressed as ratios to the abundance of aluminum. The

sample extracted from the darker, less dense layer of sediment had a higher %OC than the

sample from the lighter, denser layer (Fig. 6). Based on carbon cycling research conducted in the

fjords of Vancouver Island, the majority of organic carbon found in this area is terrigenous

(Walsh et al. 2008, Smith et al. 2015). This is partially due to the high fluxes of organic material,

transported by rivers in the steep, heavily vegetated catchments receiving, on average, over 2000

mm/yr of rainfall (Current Results). Therefore, it would seem that the darker shaded layers of

sediment are associated with larger amounts of runoff, which, in the case of Vancouver Island,

would be the winter months.

The darker layer of sediment also contained a higher abundance of sulfur, calcium, and

sodium when compared as ratios to aluminum (Fig. 6). The higher content of sulfur and calcium

can be attributed to the history of mining in the area. The currently inactive Lynx Mine in Myra

Falls, Vancouver Island, produced immense sulfide deposits, and a study done by Desbarats et al.

2005 found that the main anion and one of the dominant cations in the drainage basin of the mine

were sulfates and calcium (Desbarats et al. 2005). Because the method used to test for metals did

not remove ions from pore water, the source of sulfur detected could be from sulfate ions. This

higher abundance of sulfur and calcium in the darker shaded sediment sample would also suggest

these layers are deposited during months of higher runoff, bringing terrigenous material into the fjords.

The higher abundance of sodium in the darker segments gives credence to its terrigenous source as well. Higher concentrations of Na can be found in the sediments closest to river mouths that contain evidence of coal-operated machinery (Jonathan et al. 2003). The ash that is produced from coal-operated plants has a high Na content. Due to the extensive history of logging on Vancouver Island, it is possible that the ash produced from coal-fired machinery is the source of the higher abundance of Na in the darker shaded sediment layers (Guthrie 2002).

It is important to note that only one sample from the two shades of sediment was measured for %OC and metal composition. Although distinct differences were observed in the light and dark layers analyzed, additional samples from each sediment type would have to be analyzed in order to support the conclusions drawn with statistical significance.

Manganese & Organic Carbon

The manganese depth profile is similar in shape to an idealized depth profile of sediments deposited in an environment where oxygen is present (Fig. 9). While the methods used to test for metals did not distinguish between particulate and dissolved forms (as mentioned in the previous section), the concentrations of Mn detected are comparable to the concentrations found of particulate Mn and not dissolved Mn. As can be seen in Fig. 8, the abundance of dissolved Mn ranges from 0 to 8 ppm, while particulate can range from 0 to 6000 ppm (Crerar & Barnes 1974). Therefore, it can be assumed that the majority of the manganese measured in the Muchalat Inlet sediment was in the particulate form. The spike in Mn found at approximately 5 cm below the surface likely represents a change in the oxidation state of manganese from Mn (II) (e.g. Mn^{2+}) which is soluble in water, to Mn (III) (e.g. Mn_2O_3) or Mn (IV) (e.g. MnO_2), which are insoluble

in water (Calvert & Pederson, 1993). The manganese oxide spike is likely the result of dissolved Mn^{2+} ions from deeper in the sediment diffusing or advecting upward until reaching the oxic boundary where it becomes oxidized and reprecipitates as Mn_2O_3 or MnO_2. Thus, a spike in particulate Mn is seen at the boundary between anoxic and oxic sediment, also considered the redox boundary. This is where manganese gets "trapped" in its insoluble form as its soluble form continuously travels up toward the oxygenated zone (Libes 1992).

Because this study only has a manganese depth profile from one point in time, limited conclusions can be made. It is possible that a recent input of oxygen, such as caused by the flushing event of 2014, produced the observed Mn spike. However, without the knowledge of how manganese concentrations change with sediment depth under normal conditions, there is no way of analyzing the abnormality of this data. Therefore, the only conclusion that can be made from this manganese depth profile is that in December of 2014, the redox boundary within the sediment was at approximately 5 cm below the surface.

The depth profile of %OC represents different combinations of the light and dark layers of sediment that were partitioned from the box core (Fig. 7). The samples used to measure %OC were taken from sample bags that had been extracted from the box core at 1-2 cm increments. Hence, this process did not capture individual layers of the varve structure. Rather, it captured 1-2 cm combinations of the light and dark layers, or approximately 2-4 light layers and 2-4 dark layers within each bag based on the 0.5cm/yr accumulation rate. This can be seen when comparing the core depth with the %OC value. Every value, except for the sample from 26 cm below the surface, is composed of a %OC that falls between the %OC measured in the light layer (8%) and the %OC from the dark layer (19%).

The outlier at 26 cm below the surface visually corresponds with a thick and prominent dark layer of sediment. From the conclusions drawn about the sedimentation dynamics that produce this varve structure, a thick layer of dark shaded sediment would suggest a large flux of terrigenous material, possibly a consequence of a landslide or period of intense rainfall.
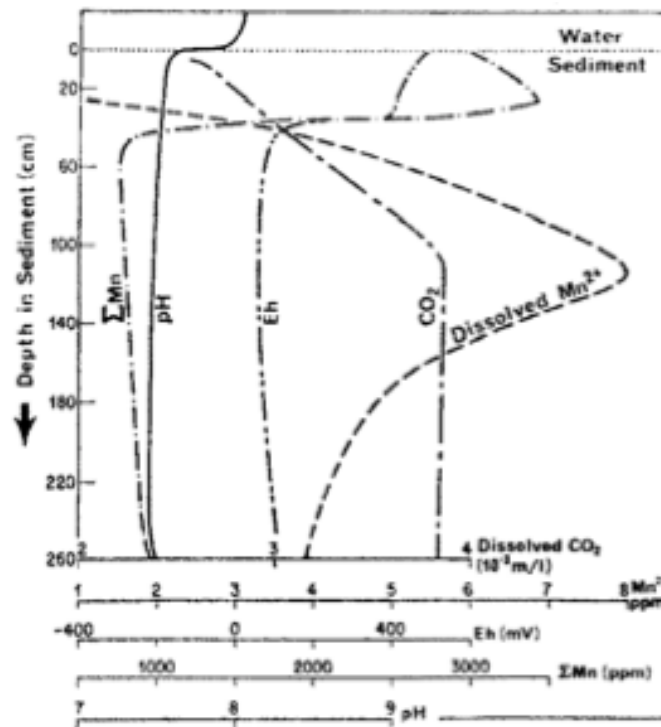

Fig. 9. An idealized geochemical depth profile of dissolved Mn^{2+}, total Mn, dissolved CO_2, pH and Eh. Source: Crerar & Barnes, 1974. The two manganese profiles display a similar shape to the profile from Muchalat Inlet, however the abundance of Mn is more comparable to the total Mn than the dissolved Mn^{2+}.

Alexandrium spp. cysts

Concentrations of *Alexandrium* spp. cysts were found in the upper 14 cm of the sediment core, however a large abundance indicative of a plankton bloom was never found (Fig. 8). The highest concentration of cysts recorded from this study was 14 cysts $* g_{dry}^{-1}$ while a bloom would show concentrations of over 100 cysts $* g_{dry}^{-1}$ (Cox et al. 2007, Feifel et al. 2012).

There are a myriad of factors that influence the concentration of cysts found in sediment. One possibility could be that once the cysts were deposited, the specific conditions of the near-

bottom environment caused the degradation of the organisms. While this is a possible explanation, the likelihood is small due to the anoxic conditions of the sediment (sulfate reducers degrade organic material at a much slower rate than do aerobes) (Pederson 1990). Additionally, if degradation had occurred, then the concentrations of the other organic constituents contained within the %OC value would be expected to have decreased as well. However, this was not the case, in fact, concentrations of some organic material actually increased further down the core. Furthermore, intact cores of *Alexandrium* spp. cysts have been observed in sediments within close proximity to Muchalat Inlet. Sediment cores from south of Nootka Sound in Sequim Bay and Saanich Inlet contain preserved cysts from the late 1800s and as far back as approximately 6000 yr BP (Mudie et al 2002, Feifel et al. 2012). Based on these variables, it can be assumed that the sediment deposited throughout the core below 14 cm was nearly absent of *Alexandrium* spp. cysts.

The physical characteristics of Muchalat Inlet and the location selected to collect the sediment core could offer further explanations for the scarcity of cyst concentrations observed. The water depth at the sediment core collection site was much deeper than the water depth of studies that found abundant cysts. A majority of the cyst records from the Puget Sound and British Columbia were from shallower settings than Muchalat Inlet. In Sequim Bay, an area of the Pacific west coast where the largest *Alexandrium* spp. cyst record has been found, cores were collected from a water depth of 27 m (Cox et al. 2008, Feifel et al. 2012). The core collected in Muchalat Inlet was collected at a water depth of 348 m. Hence, it is possible that the significantly deeper basin of Muchalat Inlet prevents resting cysts from sinking before getting carried out by currents in the upper water column. This process could be generated by tides. The close proximity of Muchalat Inlet to the Pacific Ocean causes a strong tidal signal to be detected

as far up the inlet as Gold River (Fig. 10). This prominent forcing on the upper water column

could cause a strong horizontal transport that dominates over the vertical sinking rate of the

cysts.

Based on the assumptions that resting cysts would rarely be found in sediments deposited

348 m below the surface waters, and that the concentration of cysts increased from observably

absent below 14 cm to steadily present above 14 cm, we can conclude that conditions in

Muchalat Inlet have become more conducive for *Alexandrium* spp. in recent years. Although the

concentrations found in the upper sediments do not indicate a record of plankton blooms, they do

indicate a recent arrival of the species to this inlet. Because *Alexandrium* spp. cyst records have

only been recorded in bays farther south of Muchalat Inlet (Saanich Inlet, Puget Sound, and

Sequim Bay), the recent arrival of this dinoflagellate genus could be from northern migration of
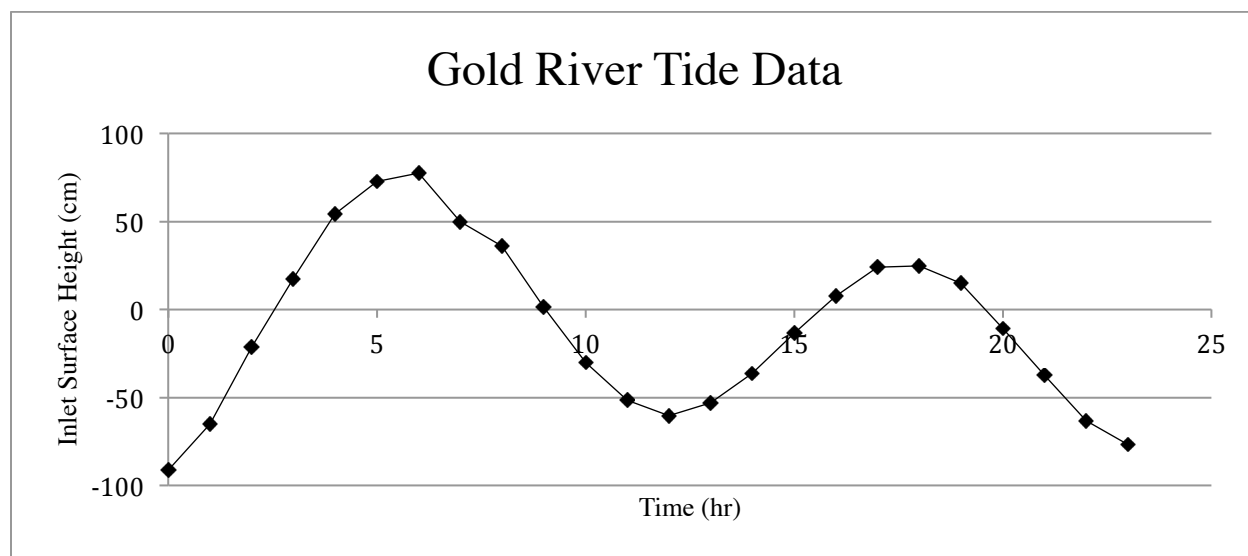
the organism.

Fig. 10. Tide data produced by Campbell Glass from the University of Washington, School of
Oceanography. This plot shows 24 hours of tide gauge data that occurred on December 14, 2014.

The recent plankton bloom from June 2014 is similar in description to the bloom from 2006 caused by *H. Akashiwo* (Almeda et al. 2010). Although the 2014 bloom did not produce the toxin that is created by *Alexandrium* spp., the record of this dinoflagellate genus produced by this study indicated recent changes to the estuarine environment of Muchalat Inlet. The results from this study would suggest that recent conditions in Muchalat Inlet have become more conducive for phytoflagellate cyst germination.

The warm anomaly that perturbed the baseline conditions of Muchalat Inlet over the spring of 2014 may have facilitated the germination of cysts and instigation of blooms. Therefore, if the observed increase in *Alexandrium* spp. cyst concentrations were due to an increase in temperature, this would align with the 2014 HAB. This conclusion is supported by the findings of Almeda et al. 2010, a study that hypothesized that the 2006 HAB was perpetrated by *H. Akashiwo* cysts that germinated due to the warmer waters.

In addition, the recent flushing event of the fjord, replenishing oxygen into deeper anoxic waters, could have upended the baseline conditions of Muchalat Inlet as well, causing a more conducive environment for cyst germination and consequentially, harmful algal blooms (Rick Keil, personal communication). Although the manganese spike could not be dated, it does indicate the presence of oxygen in the near-bottom environment, which supports the hypothesis that the flushing event aided in instigating the 2014 HAB.

CONCLUSION

It is hypothesized that the harmful plankton bloom in Muchalat Inlet from June of 2014 was most likely a result of the anomalously warm ocean water that reached the coast of Vancouver Island in May and June of 2014 (Bond et al. 2015). Based on the results from this study, it is possible that this warm anomaly perturbed the normally stratified estuarine environment of Muchalat Inlet. One of the consequences of this warmer water could be the penetration of oxygen into formerly anoxic bottom waters, causing a bioturbation of the surface sediments.

From the description of the 2014 HAB that killed over 44,000 salmon near Gold River, the cause could be the cyst-forming radiophyte, *Heterosigma Akashiwo*. Although this study cannot definitively conclude that *H. Akashiwo* was the perpetrator of the June 2014 HAB, it is plausible due to its common presence in the NE Pacific, and the fact that it was the dominant species in the 2006 bloom (Haigh & Taylor 1990, Almeda et al 2011).

Although the warm anomaly is considered an episodic phenomenon, it could also be considered a harbinger of future ocean conditions. As the climate warms, the temperature of the oceans will increase, and it is important to know how this warming will affect local ecosystems. The germination of resting cysts is a frequent stimulant for plankton blooms (Shikata et al. 2007). While this has not been a problem for environments with cold, anoxic bottom water, a warmer ocean could change deep-water oxygen levels, the consequence being an increase in cyst germination. If a warm anomaly could alter the ecosystem of the Vancouver Island fjords, then it is likely that a pervasive warming of the climate would do the same, if not more.

REFERENCES

Almeda, Rodrigo, et al. 2011. Feeding rates and abundance of marine invertebrate planktonic larvae under harmful algal bloom conditions off Vancouver Island. *Harmful Algae* 10.2: 194-206.

Average Annual Precipitation for British Columbia. *Current Results*. Retrieved May 28, 2015, from <http://www.currentresults.com/Weather/Canada/British-Columbia/precipitation-annual-average.php>.

Bond, N. A., Cronin, M. F., Freeland, H., & Mantua, N. 2015. Causes and impacts of the 2014 warm anomaly in the NE Pacific. *Geophysical Research Letters*.

Brock, F., Higham, T., Ditchfield, P., & Ramsey, C. B. 2010. Current Pretreatment Methods for AMS Radiocarbon Dating at the Oxford Radiocarbon Accelerator Unit (ORAU). *Radiocarbon, 52, 1,* 103-112.

CALIBomb. (n.d.). Retrieved May 30, 2015, from <http://www.calib.qub.ac.uk/CALIBomb/>.

Calvert, S. E., & T. F. Pedersen. 1993. Geochemistry of recent oxic and anoxic marine sediments: implications for the geological record. *Marine geology* 113.1:67-88.

Cox, A. M., Shull, D. H. & Horner, R. A. 2008. Profiles of *Alexandrium catenella* cysts in Puget Sound sediments and the relationship to paralytic shellfish poisoning events. *Harmful Algae* 7:379–88.

Crerar, D. A., & Barnes, H. L. 1974. Deposition of deep-sea manganese nodules. *Geochimica Et Cosmochimica Acta, 38, 2,* 279-300.

Dodimead, A. J., 1984. A review of some aspects of the physical oceanography of the continental shelf and slope waters off the west coast of Vancouver Island, British Columbia. *Canadian Manuscript Report of Fisheries and Aquatic Sciences* No. 1773.

Desbarats, A. J., & Dirom, G. C. 2005. Temporal variation in discharge chemistry and portal flow from the 8-Level adit, Lynx Mine, Myra Falls Operations, Vancouver Island, British Columbia. *Environmental Geology: International Journal of Geosciences, 47, 3,* 445-456.

Feifel, K. M., Moore, S. K., & Horner, R. A. 2012. An *Alexandrium* Spp. Cyst Record from Sequim Bay, Washington State, USA, and its Relation to Past Climate Variability. *Journal of Phycology*, 48(3), 550-558.

Guthrie, R. H. 2002. The effects of logging on frequency and distribution of landslides in three watersheds on Vancouver Island, British Columbia. *Geomorphology, 43, ¾,* 273

Haigh, R., & Taylor, F.J.R. 1990. Distribution of Potentially Harmful Phytoplankton Species in the Northern Strait of Georgia, British Columbia. *Canadian Journal of Fisheries and Aquatic Sciences*, 47: 2339-2350.

Horner, R. A., Garrison, D. L. & Plumley, F. G. 1997. Harmful algal blooms and red tide problems on the US west coast. *Limnology and Oceanography*. 42:1076–88.

Jonathan, M. P., Ram-Mohan, V., & Srinivasalu, S. 2004. Geochemical variations of major and trace elements in recent sediments, off the Gulf of Mannar, the southeast coast of India. *Environmental Geology Berlin,* 45, 466-480.

Judd, A. 2014. Biologist raises alarm about salmon farm in Nootka Sound. Retrieved, April 10, 2015, <http://globalnews.ca/news/1495995/biologist-raises-alarm-about-salmon-farm-in-nootka-sound/>.

Kennaway, G. M. & Lewis, J. M. 2004. An ultrastructural study of hypnozygotes of Alexandrium species (Dinophyceae). *Phycologia*. 43: 353–63.

Libes, S. M. 1992. *An Introduction to Marine Biogeochemistry*. New York: Wiley.

Meksumpun, S., Montani, S. & Uematsu, M. 1994. Elemental components of cyst walls of three marine phytoflagellates, *Chattonella antiqua* (Raphidophyceae), *Alexandrium catenella* and *Scrippsiella trochoidea* (Dinophyceae). *Phycologia*. 33:275–80

Meksumpun, S., Meksumpun, C., & Montani, S. 2005. Effects of temperature on the germination of marine phytoflagellate cysts. *Kasetsart Journal (Natural Science)*, 39(1), 149-158.

Mizushima, K., & Matsuoka, K. 2004. Vertical distribution and germination ability of *Alexandrium* spp. cysts (Dinophyceae) in the sediments collected from Kure Bay of the Seto Inland Sea, Japan. *Phycological Research*, 52, 4, 408-413.

Mudie, P. J., Rochon, A., & Levac, E. 2002. Palynological records of red tide-producing species in Canada: past trends and implications for the future. *Palaeogeography, Palaeoclimatology, Palaeoecology*, 180, 1-3.

Pedersen, T., 1990. Accumulation and preservation of organic carbon in marine sediments: The roles of anoxia vs. production. Conference: Annual convention and exposition of the American Association of Petroleum Geologists, San Francisco, CA (USA). *American Association of Petroleum Geologists*

Reimer, P. J., Brown, T. A., & Reimer, R. W. 2004. Discussion: reporting and calibration of post-bomb ^{14}C data. *Radiocarbon*, 46(3), 1299-1304.

Schumacher, B. A. 2002. Methods for the determination of total organic carbon (TOC) in soils and sediments. *Ecological Risk Assessment Support Center*, 1-23.

Shikata, T., Nagasoe, S., Matsubara, T., Yamasaki, Y., Shimasaki, Y., Oshima, Y., & Honjo, T. 2007. Effects of temperature and light on cyst germination and germinated cell survival of the noxious raphidophyte *Heterosigma akashiwo*. *Harmful Algae*, 6, 5, 700-706.

Smith, R. W., Bianchi, T. S., Allison, M., Savage, C., & Galy, V. 2015. High rates of organic carbon burial in fjord sediments globally. *Nature Geoscience,* 8, 450-453.

USEPA. 1996. USEPA 3050B: Acid Digestion of Sediments, Sludges, and Soils. SW-846 Pt 1 Office of Solid and Hazardous Wastes, USEPA, Cincinnati, OH.

Walsh, E. M., Ingalls, A. E., & Keil, R. G. 2008. Sources and transport of terrestrial organic matter in Vancouver Island fjords and the Vancouver-Washington Margin: A multiproxy approach using d13Corg, lignin phenols, and the ether lipid BIT index. *Limnology and Oceanography,* 53, 3, 1054-1063.

Wedepohl, K. H. 1971. Environmental influences on the chemical composition of shales and clays. *Physics and Chemistry of the Earth*, 8, 305-333.

Wild, E. M., Arlamovsky, K. A., Golser, R., Kutschera, W., Priller, A., Puchegger, S., Rom, W., Vycudilik, W. 2000. 14C dating with the bomb peak: An application to forensic medicine. *Nuclear Instruments and Methods in Physics Research Section B: Beam Interactions with Materials and Atoms*, 172: 944-950.

Yamaguchi, M., Itakura, S., Imai, I., & Ishida, Y. 1995. A rapid and precise technique for enumeration of resting cysts of *Alexandrium* spp. (Dinophyceae) in natural sediments. *Phycologia*, 34, 3, 207.